


# Predominant phosphorylation patterns in *Neisseria meningitidis* lipid A determined by top-down MS/MS

Constance M. John<sup>1,2</sup>, Nancy J. Phillips<sup>3</sup>, and Gary A. Jarvis<sup>1,2,\*</sup> 

<sup>1</sup>Center for Immunochemistry, Veterans Affairs Medical Center, San Francisco, CA, USA, <sup>2</sup>Department of Laboratory Medicine, University of California, San Francisco, San Francisco, CA, USA, and <sup>3</sup>Department of Pharmaceutical Chemistry, University of California, San Francisco, San Francisco, CA, USA

**Abstract** Among the virulence factors in *Neisseria* infections, a major inducer of inflammatory cytokines is the lipooligosaccharide (LOS). The activation of NF- $\kappa$ B via extracellular binding of LOS or lipopolysaccharide (LPS) to the toll-like receptor 4 and its coreceptor, MD-2, results in production of pro-inflammatory cytokines that initiate adaptive immune responses. LOS can also be absorbed by cells and activate intracellular inflammasomes, causing the release of inflammatory cytokines and pyroptosis. Studies of LOS and LPS have shown that their inflammatory potential is highly dependent on lipid A phosphorylation and acylation, but little is known on the location and pattern of these posttranslational modifications. Herein, we report on the localization of phosphoryl groups on phosphorylated meningococcal lipid A, which has two to three phosphate and zero to two phosphoethanolamine substituents. Intact LOS with symmetrical hexa-acylated and asymmetrical penta-acylated lipid A moieties was subjected to high-resolution ion mobility spectrometry MALDI-TOF MS. LOS molecular ions readily underwent in-source decay to give fragments of the oligosaccharide and lipid A formed by cleavage of the ketosidic linkage, which enabled performing MS/MS (pseudo-MS<sup>3</sup>). The resulting spectra revealed several patterns of phosphoryl substitution on lipid A, with certain species predominating. The extent of phosphoryl substitution, particularly phosphoethanolamylation, on the 4'-hydroxyl was greater than that on the 1-hydroxyl.  The heretofore unrecognized phosphorylation patterns of lipid A of meningococcal LOS that we detected are likely determinants of both pathogenicity and the ability of the bacteria to evade the innate immune system.

**Supplementary key words** bacterial membranes • glycolipids • inflammation • tandem mass spectrometry • phosphate • phosphoethanolamine • toll-like receptors • matrix-assisted laser desorption/ionization time-of-flight

The phosphorylation state and the number and length of acyl chains of the disaccharide are major factors affecting the inflammatory and immunogenic properties of the endotoxic lipid A of the lipooligosaccharide (LOS)

and lipopolysaccharide (LPS) of gram-negative bacteria. We are studying the lipid A of the pathogenic *Neisseria* that exclusively infect humans. *Neisseria gonorrhoeae* is the causative agent of gonorrhea that is a major cause of morbidity and is increasingly multidrug resistant but is asymptomatic in the majority of men and many women. *Neisseria meningitidis* is the cause of meningococcal meningitis that causes sporadic outbreaks due to localized occurrence and case clusters and, in specific regions, as epidemics. However, *N. meningitidis* also lives as a commensal organism in the human nasopharynx of 8–20% of healthy individuals who are carriers of the bacteria.

A prototypical structure of LOS from *N. meningitidis* strain 89I is shown in **Fig. 1**. The meningococcal LOS has an oligosaccharide (OS) domain with 9–12 monosaccharides consisting of two 3-deoxy-D-manno-2-octulosonic acid (Kdo) and two L-glycero-D-manno-heptose (Hep) moieties, with one or more glucose (Glc), galactose (Gal), and *N*-acetylglucosamine (GlcNAc) monosaccharides. There also are nonstoichiometric substitutions of the OS with sialic acid [*N*-acetylneuraminic acid (Neu5Ac)], acetate, glycine, and phosphoethanolamine (PEA or pEtN), which affect the biology of *N. meningitidis* (1–5). The OS domains are antigenic and some mimic human glycolipids and glycosphingolipids (6, 7). In general, the OS moiety itself is not toxic, but there is evidence that the presence of some portions of the domain, particularly the Kdo and Hep moieties, contribute to endotoxic inflammatory responses of LPS and the LOS of *N. meningitidis* (8–10).

The Neisserial lipid A domain has a largely conserved symmetrical hexa-acylated diglucosamine (GlcN) structure that is variously substituted with phosphate (P), pyrophosphate (PP), and pyrophosphoethanolamine (PPEA) and that has two to three P and one to two PEA moieties (Fig. 1). In studies to enable detailed structural analyses of the OS and of the lipid A domains of LOS and LPS, mild acid hydrolysis has been used for selective cleavage of the ketosidic bond between the OS and the lipid A, or methods employed for selective *O*-deacylation to remove *O*-linked fatty acids, or for both *O*- and *N*-deacylation of the lipid A. However, these chemical treatments can also hydrolyze biologically important labile moieties, such as the Neu5Ac,

This article contains [supplemental data](#).

\*For correspondence: Gary A. Jarvis, Gary.Jarvis@ucsf.edu.

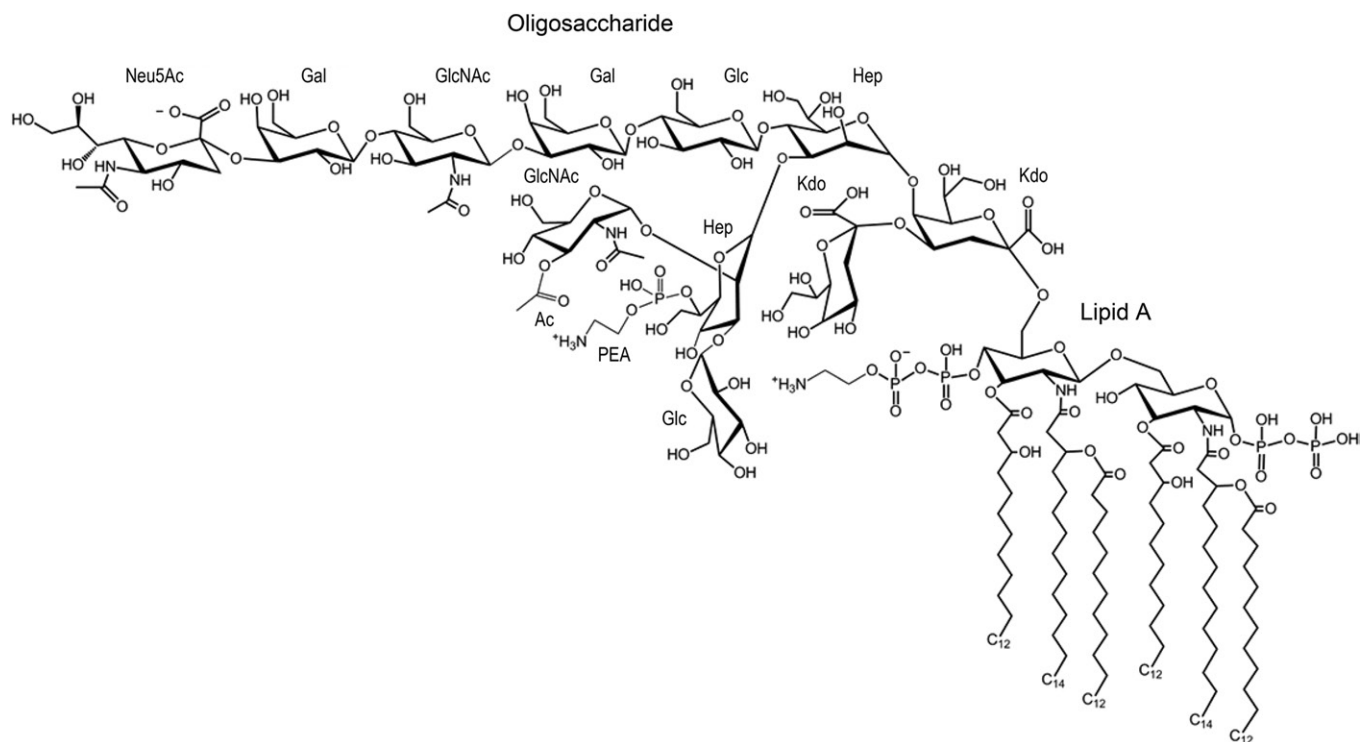


**Fig. 1.** Illustration of the LOS from 89I showing an OS moiety with a composition of two Hep, two Kdo, two GlcNAc, two Gal, two Glc, PEA, OAc, and Neu5Ac. The lipid A shown has a reducing terminal PP moiety and a PPEA moiety on the nonreducing terminus.

acetate, glycine, and phosphoryl groups (11, 12), which has hampered the detection of these substituents and discernment of their bioactivity.

We have adopted methods for top-down analysis of intact LOS using MALDI-TOF MS/MS to better enable structural and quantitative determination. Using this approach, we have shown that lipid A from both *N. meningitidis* and *N. gonorrhoeae* is substituted to varying extents with PP groups and PPEA groups (12). Pyrophosphorylation of lipid A has also been reported in LOS from some other gram-negative bacteria (13). In studies using human monocytes, we found that greater abundance of lipid A phosphorylation and phosphoethanolaminylation was correlated with increased inflammatory potential of the intact LOS and the whole bacteria (12, 14–16). We also found that removal of all P groups from *Escherichia coli* O55:B5 LPS and *N. meningitidis* 89I LOS by hydrogen fluoride treatment significantly reduced inflammatory signaling in human monocytic cells (14).

The reducing terminal 1-position P on lipid A is present as a consequence of the LpxH-mediated cleavage of the lipid A precursor originally formed from UDP-GlcNAc. The enzyme LpxK transfers P from ATP to the 4'-position on the nonreducing terminal GlcN during lipid A biosynthesis.

EptA (previously termed LptA) is the ethanolamine transferase that transfers PEA from phosphatidylethanolamine to lipid A (17). The expression of *eptA* by the pathogenic *Neisseria* has been found to be strain variable. It is translationally regulated by phase variation in the open reading frame and its stabilization by oxidoreductases, and

is transcriptionally regulated by the PmrA/PmrB two-component system that is responsive to pH, the concentration of  $Mg^{2+}$ ,  $Fe^{2+}$ , and  $Al^{3+}$ , and cationic antimicrobial peptides. In addition, *eptA* is subject to indirect regulation by the PhoP/PhoQ two-component system (18–20).

Functional orthologs of *lpxT*, which encodes an enzyme that transfers P to the 1-position of bis-phosphoryl lipid A, have been identified in gram-negative species, including *E. coli*, *Salmonella enterica*, and *Pseudomonas aeruginosa* (21–23) but not in *Neisseria*, despite its expression of pyrophosphoryl lipid A. There is evidence in *E. coli* that the P-specific transport system regulates expression of *lpxT*, and recent data show that its activity in *P. aeruginosa* is increased by higher concentrations of magnesium (22, 24). Very little is known about the control of pyrophosphorylation in *N. meningitidis* and *N. gonorrhoeae*, but our data showing stable strain-specific phosphoryl substitution of the lipid A indicates that there is some type of strain-variable regulation (12, 15, 25).

The mechanism that leads to an increase in inflammatory signaling with more pyrophosphorylation of meningococcal lipid A is also unclear. Potential mechanisms that have been proposed include lessening of the effect of the net ionic charge of the lipid A with pyrophosphorylation due to coulombic repulsion or that pyrophosphorylation could affect an unrelated aspect of the bacteria that is important in its survival, such as outer membrane stability (26). Crystallography has revealed that basic amino acids of the extracellular toll-like receptor 4 (TLR4)/MD-2 complex bind to 1- and 4'-position P moieties of bis-phosphoryl lipid A and facilitate TLR4/MD-2 dimerization that leads

to intracellular signaling via MyD88-dependent and -independent pathways (25, 27–29). It has been shown that the meningococcal LOS and lipid A induce TLR4/MD2 signaling by both intracellular pathways (15, 30). However, the relative ability of specific highly phosphorylated lipid A molecules to induce intracellular signaling by the two pathways or to interact with amino acids in the TLR4/MD-2 complex is unknown.

Intracellularly, the LOS of *N. gonorrhoeae* recognizes and activates inflammasomes, which are intracellular pattern-recognition receptor signaling effectors (31). When activated, the canonical NLRP3 inflammasome induces the secretion of IL-1 $\beta$  and IL-18 as well as pyroptotic cell death. In monocytes and epithelial cells, LPS activates inflammasomes by binding to and activating human caspase-4 and caspase-5 (32, 33).

There is a body of evidence that shows phosphoethanol-amination of the lipid A of LOS uniquely affects its bioactivity by reducing the net negative charge of lipid A. The presence of a PEA on lipid A confers resistance to mediators of innate host defense including endogenous and exogenous cationic antimicrobial peptides such as polymyxin B. In meningococci, phosphoethanolamination of lipid A increases resistance to complement-mediated killing by normal human serum (34–37). The presence of PEA on lipid A has also been found to enhance adhesion of unencapsulated meningococci to human endothelial and epithelial cells (38). Our previous studies have shown that most nonpathogenic commensal *Neisseria spp.* express bis-phosphoryl lipid A lacking both phosphoethanolamination and pyrophosphorylation and do not express a functional *eptA* gene. We also found that bacteria and LOS produced by a knockout strain of *N. meningitidis* 7946 lacking *eptA* expression had reduced inflammatory potential (16).

There is evidence that the localization of phosphoryl groups on the 1-position compared with the 4'-position of the nonreducing terminal GlcN is a determinant of the inflammatory potential of lipid A from some species of gram-negative bacteria (39–41). For example, the human commensal *Bacteroides thetaiotaomicron* expresses penta-acylated lipid A with a single P on the 1-position and is a human TLR4 agonist, whereas the penta-acylated lipid A from the pathogenic *Porphyromonas gingivalis* has a single P on the 4'-position, but does not induce human TLR4 signaling (42). Furthermore, penta-acylated lipid A from mutant forms of monophosphoryl *E. coli* with a 1-P is more immunostimulatory than the same lipid A with a 4'-P (39). Results showing that a bis-P hexa-acylated lipid A from *Erwinia carotovora* induced significantly more TNF- $\alpha$  in human peripheral blood mononuclear cells compared with the hexa-acylated lipid A with only a 4'-P were also indicative of the greater inflammatory potential of P on the 1-position (43).

The significance of lipid A phosphorylation, its localization, and inflammatory potential are well illustrated by monophosphoryl lipid A (MPLA), which is a modified hexa-acylated form of lipid A from *Salmonella minnesota* with only a single 4-P that has immunostimulatory activity but much less inflammatory potential than the wild-type bis-phosphoryl lipid A that also has a 1-position P. Unlike

bis-phosphoryl lipid A, it was shown that MPLA engages the TLR4-MD2 complex, but this results in downstream activation of the TRIF-TRAM signaling pathway only without inducing the MyD88-Mal pathway (41). MPLA has been successfully developed as an adjuvant in vaccines for hepatitis B, melanoma, and human papilloma virus (40, 41).

Although the localization of P substituents on lipid A clearly has been shown to be biologically significant, it has not been analyzed in lipid A from pathogenic *Neisseria spp.* Therefore, we undertook the analysis of the substitution of the 1- and 4'-position of lipid A with P and PEA using the techniques that we have adopted for top-down analysis of intact LOS using MALDI-TOF MS/MS (44). In this approach molecular ions of intact LOS were produced and readily underwent a type of in-source decay that occurs at the sample surface in a few pico- to nanoseconds before or during desorption, to give gas phase fragments from cleavage of the labile ketosidic linkage. This enabled collision-induced dissociation (CID) of lipid A fragment ions formed by in-source decay to obtain MS/MS spectra that represent pseudo-MS<sup>3</sup> analyses. Ion mobility spectrometry (IMS) was used to cleanly select parent ions of a lipoidal nature for the MS/MS (IMS-MS/MS) using a Synapt G2 high-definition mass spectrometer (HDMS). We analyzed LOS from meningococcal strains that produced the hexa-acylated lipid A that is characteristic of most *Neisseria spp.* and LOS from a naturally occurring *lpxL1* mutant strain that produced a penta-acylated lipid A, which, being inherently asymmetrical, facilitated the unambiguous identification of fragment ion peaks as being of reducing terminal or nonreducing terminal origin. Examination of the spectra from the hexa-acylated and penta-acylated lipid A revealed that several patterns of phosphoryl substitution on the lipid A could be detected with specific species predominating. Our results reveal the structural complexity due to heterogeneity in phosphorylation of the meningococcal lipid A and highlight the need for complete structural analyses to accurately decipher the relationship between the structure of lipid A and its bioactivity and inflammatory potential.

## MATERIALS AND METHODS

### Bacterial strains and LOS preparation

*N. meningitidis* serogroup C strain 89I is a clinical isolate that has been described previously (25, 45). *N. meningitidis* serogroup B strain 701 and serogroup Y *lpxL1* mutant strain 399 are isolates from throat cultures of carriers of *N. meningitidis* without disease, and serogroup B isolate 90/90 is from an infected person obtained during a serogroup B vaccination trial in Norway (46–48). We have recently characterized the LOS from a large sampling of invasive and carrier Norwegian strains of *N. meningitidis* in order to correlate clinical outcomes with LOS structural features (5). LOS from all strains was extracted and purified by a modification of the hot phenol-water method (49, 50).

### Preparation of intact LOS for analysis by MALDI-TOF MS

As we have previously reported, intact LOS was deposited on a prespotted matrix layer for MALDI-TOF MS (12, 14, 16, 51). The matrix was prepared by mixing a 3:1 (v/v) ratio of a solution of

2',4',6'-trihydroxyacetophenone (200 mg/ml in methanol; Sigma-Aldrich) with a solution of nitrocellulose transblot membrane (15 mg/ml in acetone/isopropanol, 1:1; Bio-Rad) that produced thicker matrix layers than in the original protocol (52) optimized for analysis on the Synapt G2 HDMS. Aliquots of the matrix solution (~1  $\mu$ l) were spotted on a stainless-steel sample plate and air dried. Intact LOS (4–10 mg/ml) was suspended in methanol/water, 1:3, containing 5 mM EDTA, and aliquots were desalted with a few cation-exchange beads (Dowex 50WX8-200) that had been converted to the ammonium form. Desalted LOS solutions were mixed 9:1 (v/v) with 100 mM dibasic ammonium citrate, and ~1  $\mu$ l aliquots were deposited on the dried matrix spots and air dried.

### Negative-ion MALDI-TOF MS analyses of intact LOS

MALDI-TOF MS was performed in an instrumental “sensitivity mode” on a Synapt G2 HDMS (Waters Corporation, Manchester, UK) equipped with a Nd:YAG laser set to 355 nm wavelength with a 200 Hz firing rate. The sensitivity mode employs broader selection conditions that are designed to optimize sensitivity. Spectra generally were acquired for ~1–2 min, with a scan of 1.0 s and cycle time of 1.024 s. MassLynx 4.1 software was used to digitally smooth and correct the baseline of spectra. Calibration was performed with masses of the monoisotopic (M-H)<sup>-</sup> ions for bovine insulin at  $m/z$  5,728.5931, insulin B-chain at  $m/z$  3,492.6357, renin substrate at  $m/z$  1,756.9175, and angiotensin II at  $m/z$  1,044.5267 (all from Sigma-Aldrich). The isotopically resolved peaks are labeled with their monoisotopic masses (<sup>12</sup>C-only containing species).

### Negative-ion IMS-MS and IMS-MS/MS analyses of intact LOS

IMS was performed on a Synapt G2 HDMS equipped with a T-wave ion mobility cell (Triwave™) (53, 54), operating in MALDI mode. The T-wave device consists of three cells; a Trap cell, an IMS cell, and a Transfer cell. For IMS-MS experiments, the T-wave peak height voltage was 40 V and the T-wave velocity used was generally a variable wave velocity of 650–250 m/s. Typically, the T-wave mobility cell contained nitrogen at a pressure of ~2 mbar, trap gas flow was 0.4 ml/min, helium cell gas flow was 180 ml/min, IMS gas flow was 90 ml/min, and trap DC bias was 80 V. In IMS mode, spectra were typically acquired for 1–2 min, with scanning parameters as noted above.

For analysis of lipid A fragment ions in IMS-MS/MS experiments, collision energy was applied in the Transfer cell following IMS, at values ranging from 50 to 90 V, depending on the analyte. The Transfer cell contained argon as the collision gas. A T-wave variable wave velocity of 1,100–200 m/s was used. Precursor ions were selected with instrument LM and HM resolution settings of 4.7 and 15.0, respectively. Two-dimensional IMS spectra were viewed using DriftScope 2.1 software, and selected spectral regions were exported to MassLynx with retention of drift time information for generation of mobilograms and subspectra. The nomenclature used in labeling the fragment ions is presented in Fig. 2.

## RESULTS

### Analyses by IMS-MS/MS

All MS/MS spectra presented were produced using IMS resolution of plumes of intact LOS ions from plumes of fragment ions of lipid A and OSs. The value of the IMS resolution (Fig. 3A, B) is illustrated (Fig. 3C). For example,

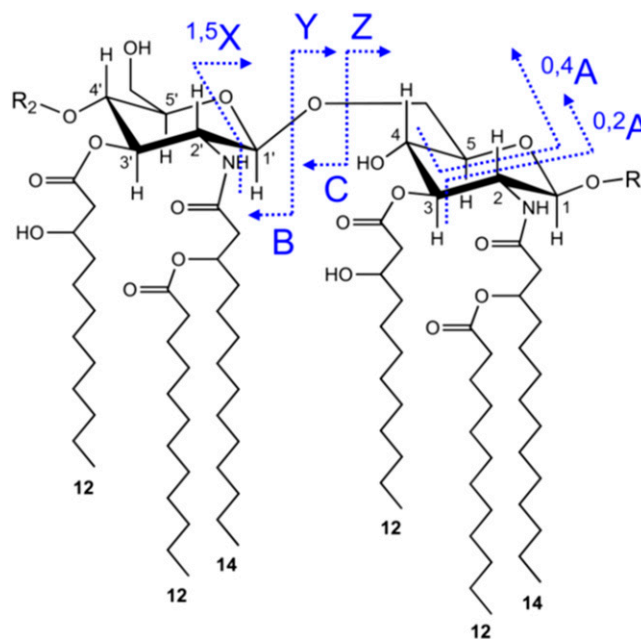


**Fig. 2.** The origin and nomenclature used for glycosidic and cross-ring fragment ions of the lipid A that are observed in MS/MS or MS<sup>n</sup> analyses. As indicated, fragment ions with charge retention on the nonreducing terminus are termed A-, B-, or C-type ions, whereas fragment ions with charge retention on the reducing terminus are X-, Y-, or Z-type ions. B-, C-, Y-, and Z-type ions arise from glycosidic bond cleavages, whereas A- and X-type fragments are cross-ring cleavages. Fragment ions of the B- and C-type differ by 18 Da (water), as do Y- and Z-type fragments. In the nomenclature used for cross-ring fragment ions (A- and X-type), the atoms that were forming the broken bond are included in the name. For example, as shown, <sup>0,4</sup>A ions result from cleavage of the bond between the glycosidic oxygen (0) and the first carbon (1), and the fourth (4) and fifth (5) carbon on the glycosidic ring. This nomenclature is widely used in MS analyses of carbohydrates and was first proposed by Domon and Costello (57).

the peak for lipid A fragment ions at  $m/z$  1,555.01 can be completely resolved from the base peak in the spectrum for the OS fragment ions at  $m/z$  1,554.53. The clean separation afforded by IMS enabled more unambiguous identification of fragment ions in the IMS-MS and MS/MS spectra.

### Phosphorylation states of hexa-acylated and penta-acylated lipid A from meningococcal LOS

In our MALDI-TOF MS (non-IMS) of fragment ions from lipid A of hexa-acylated or penta-acylated intact LOS from *N. meningitidis* produced by in-source decay, we detected five main types of molecules in terms of phosphoryl compositions (Fig. 4A and B, respectively). Specifically, prominent peaks for fragment ions produced by in-source decay were observed for hexa-acylated and penta-acylated lipid A molecules with: *i*) 3P PEA at  $m/z$  1,915.17 and  $m/z$  1,732.96; *ii*) 2P PEA at  $m/z$  1,835.20 and  $m/z$  1,652.99; and *iii*) 3P at  $m/z$  1,792.15 and  $m/z$  1,609.95. Prominent peaks were also observed at  $m/z$  1,737.25 and at  $m/z$  1,555.01 due to the facile loss of 2P (H<sub>4</sub>P<sub>2</sub>O<sub>7</sub>, 177.94 Da) from 3P PEA lipid A, which is consistent with previous observations of this fragmentation in MS/MS analyses of lipid A (13). Ions for the most highly phosphorylated 3P 2PEA lipid A at  $m/z$

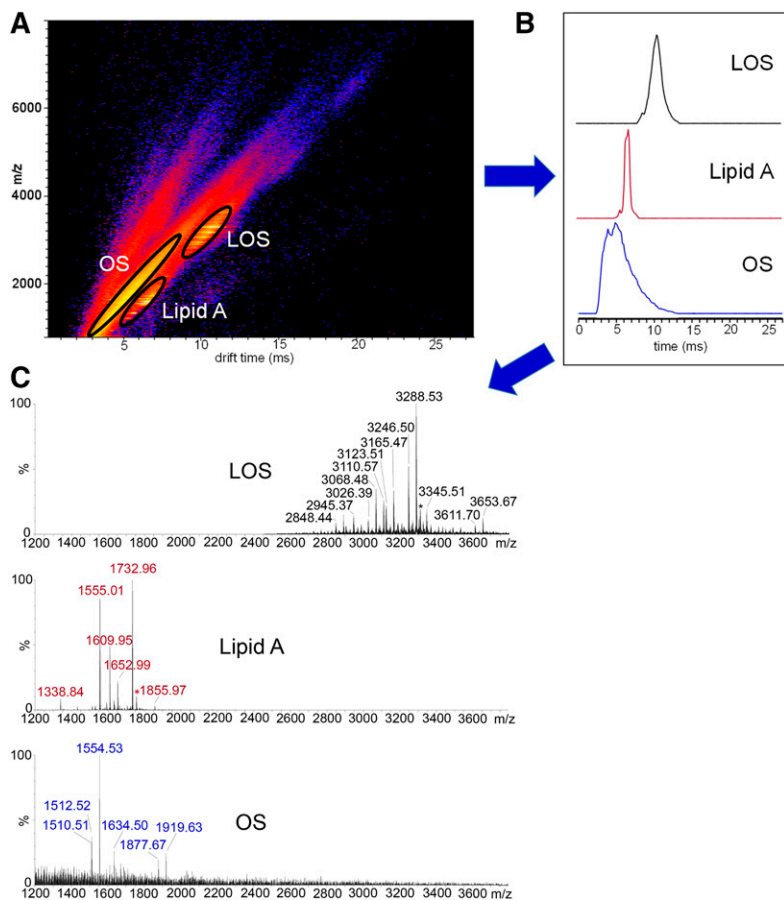


**Fig. 3.** Analysis of intact LOS from *N. meningitidis* strain 399 by MALDI-TOF MS with IMS. The two-dimensional plot of the IMS data (DriftScope heat map) shows as indicated the clean resolution of the ion plumes for the intact LOS ( $M-H$ )<sup>-</sup> ions from fragment ions of OS and lipid A produced from in-source decay (A). Circled regions were selected, and the data were exported to MassLynx with the drift time retained to create the corresponding mobilograms (B). The spectra of the extracted LOS ( $M-H$ )<sup>-</sup> ions and OS and lipid A ions are shown (C). The MALDI-TOF MS produced baseline separation of peaks differing by 1 Da, and the masses presented are monoisotopic masses of isotopically resolved peaks of <sup>12</sup>C-only-containing molecules.

2,038.26 and 1,855.97 were in low abundance and, for this reason, were not subject to further analysis by MS/MS. There were no significant peaks for lipid A with 2P 2PEA substitution in either spectrum, which was previously

reported as the major phosphoform of meningococcal lipid A in a different strain of *N. meningitidis* (55). These data (Fig. 4) and our previous MS analyses indicate that, in terms of phosphoryl groups, the biosynthesis of Neisserial

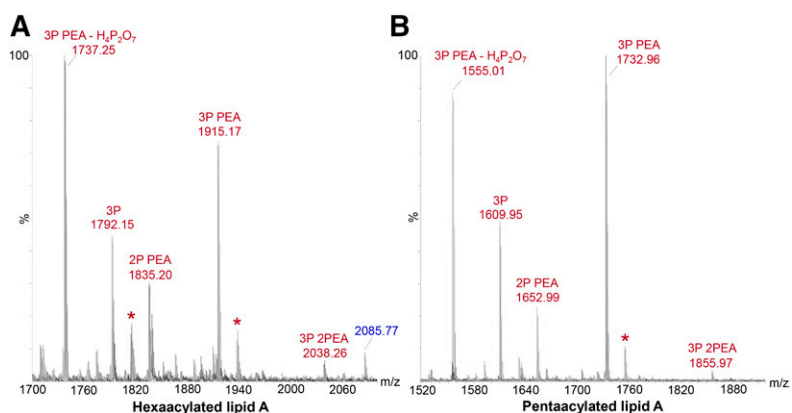


**Fig. 4.** Negative-ion MALDI-TOF (non-IMS) spectra of intact LOS from *N. meningitidis* strain 90/90 (A) and strain 399 (B), which is a *lpxL1* mutant strain, showing regions containing peaks for lipid A fragment ions produced by in-source decay. In the spectrum of 90/90 LOS (A) peaks for hexaacylated lipid A fragment ions with three P and two PEA groups can be observed at  $m/z$  2038.26. Analogous peaks with three P and two PEA groups can be observed in the spectrum of 399 LOS (B) for penta-acylated lipid A that is lacking a laurate group on the nonreducing terminal glucosamine at  $m/z$  1,855.97. More prominent peaks can be observed for fragment ions of lipid A with either two or three Ps and a single PEA moiety and three Ps. The prominent peaks at  $m/z$  1,737.25 (A) and 1,555.01 (B) are most likely due to the facile loss of  $H_4P_2O_7$  from fragment ions at  $m/z$  1,915.17 and 1,732.96, respectively, for lipid A with three P substituents and one PEA substituent. Peaks denoted with asterisks represent sodiated fragment ions ( $M-H_2+Na$ )<sup>-</sup>. The peak at  $m/z$  2,085.77 labeled in blue-colored font (A) is from OS fragment ions.

LOS results in a mixture of lipid A molecules. We have found that increased fragmentation of P and PEA groups can occur in MALDI-TOF MS with increased laser power, and, therefore, we kept it as low as possible (5, 44).

### IMS-MS/MS of hexa-acylated and penta-acylated 3P PEA lipid A

The fatty acid substitution of hexa-acylated lipid A from *N. meningitidis* is symmetrical. Therefore, it is not possible to unambiguously distinguish nonreducing terminal C- or B-type ions from reducing terminal Y- or Z-type ions, respectively, due to their identical compositions. Penta-acylated lipid A molecules from the *lpxLI* isolates lack the lauric acid moiety linked to the  $\beta$ -3 hydroxy-*N*-myristate moiety on the nonreducing terminal glucosamine and, thus, are inherently asymmetrical (5, 56). The relative abundances of ions in the spectra in Fig. 4 for penta- and hexa-acylated lipid A molecules with the same phosphoryl compositions are similar, which indicates that the phosphorylation state of the hexa-acylated and the penta-acylated lipid A molecules is similar. Therefore, to determine the localization of phosphoryl groups, we acquired and examined spectra from IMS-MS/MS of asymmetrical penta-acylated lipid A ions to inform our interpretation of IMS-MS/MS spectra of the symmetrical hexa-acylated lipid A.

Separation of ions in IMS depends on molecular size, shape, and charge. The mobilogram (Fig. 5B) illustrates the clean separations that we obtained of OS and lipid A fragment ions upon selection of lipid A ions at  $m/z$  1,915.1 for CID. Traveling ahead of the lipid A species, the fragment ions at  $m/z$  1,924.64 appearing in our selection window (Fig. 5C) are consistent with  $-43.99$  Da ( $-\text{CO}_2$ ) from OS fragment ions at  $m/z$  1,968.6 corresponding to a composition of two Hep, two Kdo, HexNAc, three Hex, PEA, OAc, and Neu5Ac that was previously reported (5). Fragment ion peaks in accord with this assignment can be observed at  $m/z$  1,704.80 for  $-\text{Kdo}$  ( $-220.06$  Da), at  $m/z$  1,633.57 for  $-\text{Neu5Ac}$  ( $-291.10$  Da), and at  $m/z$  1,413.46 for loss of both Kdo and Neu5Ac. These otherwise interfering OS fragment ions are completely resolved from the lipid A fragment ions of interest using IMS-MS/MS.

We acquired and analyzed negative-ion IMS-MS/MS spectra from CID of lipid A fragment ions produced by in-source decay of LOS from strain 89I (Fig. 5D), strain 701 (Fig. 5G), and the penta-acylated *lpxLI* mutant strain 399 (Fig. 5H). The peaks for 3P PEA lipid A ions at  $m/z$  1,915.1 (arrow, Fig. 5D, G) and  $m/z$  1,733.0 (arrow, Fig. 5H) were subject to CID. In the MS/MS spectra, there are prominent peaks formed by losses of P and PEA and/or fatty acids as well as peaks for Y- and B-type fragment ions of the GlcN. The labeling of the glucosamine fragment ions in the spectra and corresponding structures (Fig. 5A, E, F, I) are based on the classifications of Domon and Costello (57).

Color-coding was used to associate fragment ions with the structures of the molecules proposed to be the source of fragment ions. For example, red-colored font in the labels for the  $m/z$  values of fragment ions in the spectra is

indicative of ions that were uniquely consistent with the red-colored molecule (Fig. 5A) having 2P on the reducing terminus and a P PEA substituent on the nonreducing terminus. The green boxes shown around the  $m/z$  values of the fragment ions on the structures and in the spectra (Figs. 5–7, supplemental Fig. S1) indicates these were specific for penta-acylated *lpxLI* mutant lipid A molecules with the same phosphoryl substitution pattern but lacking the laurate groups that are drawn in green on the structures.

There are prominent peaks for fragments of the  $(\text{M-H})^-$  ions that lost P (79.97 Da), PEA (123.01 Da), 2P, and P PEA in all three spectra of lipid A (Fig. 5D, G, H). In addition, fragment ions due to loss of *O*-linked acyl chains are observed. Hexa-acylated Neisserial lipid A (Fig. 5A, E, F, I) has two *O*-linked laurate (C12:0) and two 3- $\beta$  hydroxylaurate (C12:0 3-OH) groups, which can be cleaved as alkane carboxylic acids ( $-200.18$  and  $-216.17$  Da) or alkyl ketenes ( $-182.17$  and  $-198.16$  Da), respectively.

The base peaks in the MS/MS spectra were observed at  $m/z$  1,737.2 (Fig. 5D, G) and at  $m/z$  1,555.0 (Fig. 5H) due to the facile loss of  $\text{H}_4\text{P}_2\text{O}_7$  molecules, as observed in the MS spectra above (Fig. 4A, B). The second most prominent peak in each of the lipid A spectra is for Y-type fragment ions at  $m/z$  944.5. Nonreducing terminal B-type ions at  $m/z$  969.5 and  $m/z$  787.5 were also relatively prominent in the spectra of the hexa-acylated (Fig. 5D, G) and penta-acylated (Fig. 5H) lipid A, respectively. The other less abundant Y-type fragment ions observed were at  $m/z$  1,067.57 for fragment ions with 2P PEA substituents on the reducing terminus in the spectra of strains 701 and 399 (Fig. 5G, H).

Although less prominent than the peaks observed for the Y-type fragment ions, there were observable peaks for nonreducing B-type ions corresponding to all four of the proposed structures for the variously phosphorylated hexa-acylated lipid A (Fig. 5A, E, F, I). Peaks at  $m/z$  1,049.5, 969.6, 926.5, and 846.6 for B-type ions represent structures with nonreducing terminal 2P PEA, P PEA, 2P, and P substituents, respectively (Fig. 5D, G). The presence of 2P PEA groups on the lipid A was indicated by the low mass peaks in the three spectra for 2P PEA at  $m/z$  299.9 (Fig. 5D, G, H). The peak at  $m/z$  846.6 for a lipid A with nonreducing terminal P and reducing terminal 2P PEA was observed only in the spectrum of strain 701 (Fig. 5G). However, the presence of 2P PEA on the reducing terminus was also supported by the Y-ion peaks at  $m/z$  1,067.6 in the spectrum of strains 701 and 399 (Fig. 5G, H).

The most prominent peaks for B-type ions of hexa-acylated lipid A were at  $m/z$  1,049.5 for nonreducing terminal 2P PEA fragment ions. The next most prominent were peaks at  $m/z$  969.5 for P PEA on the nonreducing terminus (Fig. 5D, G). B-ions for nonreducing terminal hexa-acylated lipid A molecules with 2P substituents at  $m/z$  926.6 were less abundant. Even fewer ions were detected at  $m/z$  846.6 for molecules with a single nonreducing terminal P substitution. Thus, the relative prominence of peaks for B-ions appeared to be at least partly due to differences in the capacity for negative-ion charge retention on the nonreducing terminus.

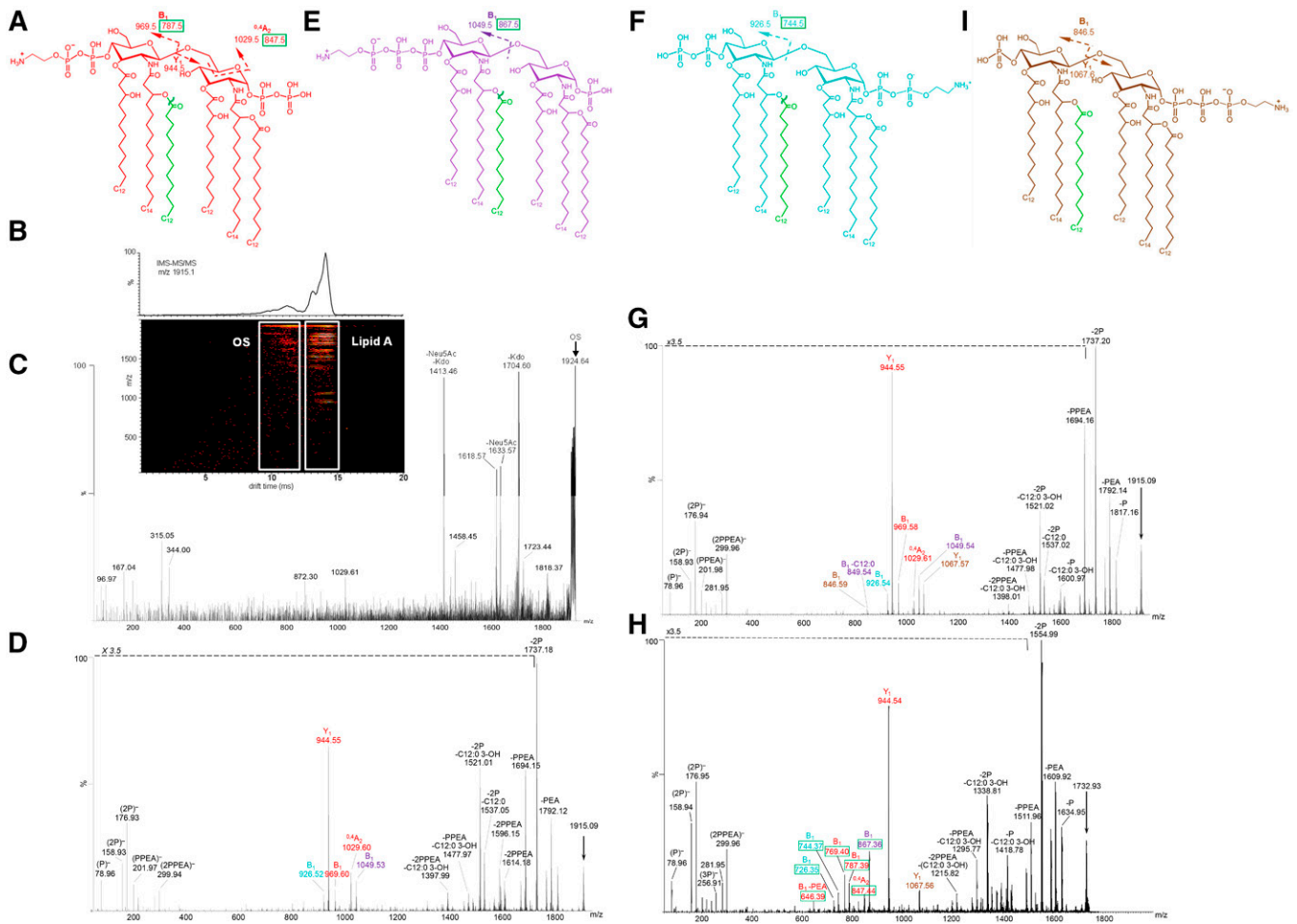


**Fig. 5.** Structures A, E, F, and I are in accord with the lipid A fragment ions detected in the negative-ion MALDI-TOF IMS-MS/MS spectra presented of fragment ions of 3P PEA lipid A at  $m/z$  1,915.1 (arrows) from intact LOS of strain 891 (D), of strain 701 (G), and at  $m/z$  1,732.9 (arrow) from the 399 *lipxL1* (H) mutant strain. The major fragment ions of lipid A that are informative regarding the localization of phosphoryl groups are labeled and shown on the spectra and related structures. Peaks for fragment ions due to cleavage of more than one bond are labeled in the spectra with notations for the multiple mechanisms. Colors that are used for the fonts designating the  $m/z$  values and the type of fragment ions observed are the same as the color of the structure that we propose produced the fragmenting ions. Each of the structures illustrated is designed to represent the phosphoform of both the hexa-acylated and the penta-acylated lipid A. The green-colored laurate that is shown on each of the structures is that which is lacking in lipid A of the *lipxL1* mutant strain 399. The green boxes around masses of fragment ions on the structures and in the spectrum of the 399 lipid A (H) are used to identify the fragment ions arising from the penta-acylated lipid that is lacking the green-colored laurate. The CID was performed in the Transfer region of the Triwave device after IMS separation and the MS/MS spectra were selected from two-dimensional plots, as illustrated for strain 701 in the panel (B), which presents the total ion mobilogram above the plot of IMS-MS/MS data. The instrumental sensitivity mode that was used permitted the transmission of interfering OS fragment ions in the selection window (C), but these were easily resolved from lipid fragment ions by IMS.

Only a few peaks for ions formed by cross-ring fragmentation were detected. These were for  $^{0,4}A_2$ -type nonreducing terminal fragment ions of hexa-acylated lipid A at  $m/z$  1,029.5 (Fig. 5D, G) and for the analogous  $^{0,4}A_2$ -type ions of the penta-acylated lipid A at  $m/z$  847.5 (Fig. 5H). The peaks for the  $^{0,4}A_2$ -type and nonreducing terminal B-type fragment ions in the MS/MS spectra provided more evidence for reducing terminal substitution with P, 2P, and P PEA relative to 2P PEA. However, peaks for some corresponding Y-type reducing terminal ions were not observed. Thus, observation of B-type ions was critical in establishing the presence of the variously phosphorylated lipid A molecules.

In the MS/MS spectrum of the penta-acylated 3P PEA lipid A (Fig. 5H), there were significant peaks for nonreducing

terminal B-type ions with the most abundant ions for 2P PEA groups at  $m/z$  867.4, which corresponded to the most prominent peaks for B-type ions of hexa-acylated lipid A at  $m/z$  1,049.5. B-type fragment ions with P PEA groups at  $m/z$  787.5 were less abundant. The smallest peak was at  $m/z$  744.4 for B-type fragment ions with 2P substitution. The spectrum of the penta-acylated lipid A lacked a significant peak for B-type ions with a single P group, analogous to the least abundant of the B-type ions of the hexa-acylated lipid A at  $m/z$  846.6 (Fig. 5G). In the negative ion spectra, charge retention would be expected to increase on termini with more P groups, and this would increase the relative abundance of corresponding Y- or B-type ions generally. Overall, the relative abundance of B-type ions in the three MS/MS spectra of 3P PEA lipid A indicated that the nonreducing

termini were more highly phosphorylated, particularly with PEA groups, compared with the reducing termini.

### IMS-MS/MS of hexa-acylated and penta-acylated 2P PEA lipid A

In MS/MS spectra of the 2P PEA lipid A at  $m/z$  1835.2 from strain 89I (Fig. 6A) and strain 701 (Fig. 6B) and at  $m/z$  1653.0 from the *lpxL1* mutant 399 strain (Fig. 6D), fragment ions provided evidence for nonreducing terminal P PEA and 2P PEA substitution, with one or no P on the reducing terminus, respectively. Lipid A ions at  $m/z$  1,835.2 (arrow, Fig. 6A, B) and  $m/z$  1,653.0 (arrow, Fig. 6D) were subjected to CID. There were prominent peaks observed for losses of P and PEA and/or fatty acids and for B- and  $^{0,4}A_2$ -type fragment ions with nonreducing terminal P PEA substituents at  $m/z$  969.6 and 1,029.6 in the spectra of the hexa-acylated lipid A (Fig. 6A, B) and at  $m/z$  787.4 and 847.4 in the spectrum of the penta-acylated lipid A (Fig. 6D). Less prominent peaks were observed for B-type ions with nonreducing terminal 2P PEA substituents at  $m/z$  1049.58 (Fig. 6B) and 867.36 (Fig. 6D) in the spectra of the hexa-acylated and penta-acylated lipid A, respectively. However, we did not detect ions consistent with P PEA substitution of the reducing terminus as indicated in the proposed structures (Fig. 6C, E) despite the occurrence of peaks consistent with reducing terminal PEA in the MS/MS of the 3P PEA lipid A (Fig. 5). These findings indicate that the nonreducing

terminus is more phosphoethanolaminylated than the reducing terminus of the lipid A.

### IMS-MS/MS of hexa-acylated and penta-acylated 3P lipid A

In the spectra of the 3P lipid A from strain 701 (Fig. 7B) and the 399 *lpxL1* mutant strain (Fig. 7D), peaks for both Y-type and B-type fragment ions were observed along with prominent peaks due to losses of phosphoryl substituents and/or fatty acids. Peaks for Y-type fragment ions were observed at  $m/z$  944.6 and 864.6, which had only a single P substituent. Observation of the B-type ions on hexa-acylated lipid A at  $m/z$  1,006.5, 926.6, and 846.6 enabled localization of the 3P, 2P, and P groups on the nonreducing termini (Fig. 7B). The B-type fragment ions of penta-acylated lipid A peaks at  $m/z$  824.4 and 744.4 revealed the presence of nonreducing terminal 3P and 2P (Fig. 7D). The most abundant B-type fragment ion peaks were at  $m/z$  926.6 (Fig. 7B) and 744.4 (Fig. 7D) that were consistent with the aqua-colored structure (Fig. 7A) with 2P on the nonreducing termini. Less prominent peaks were for nonreducing terminal B-type fragment ions with 1P or with 3P, which were observed at  $m/z$  846.6, consistent with the brown-colored structure (Fig. 7E), and at  $m/z$  1006.5 (Fig. 7B) and 824.3 (Fig. 7D), in accord with the novel 1-dephospho-4'-trisphosphate structure shown in pink-color (Fig. 7C). The presence of the latter structure was also supported

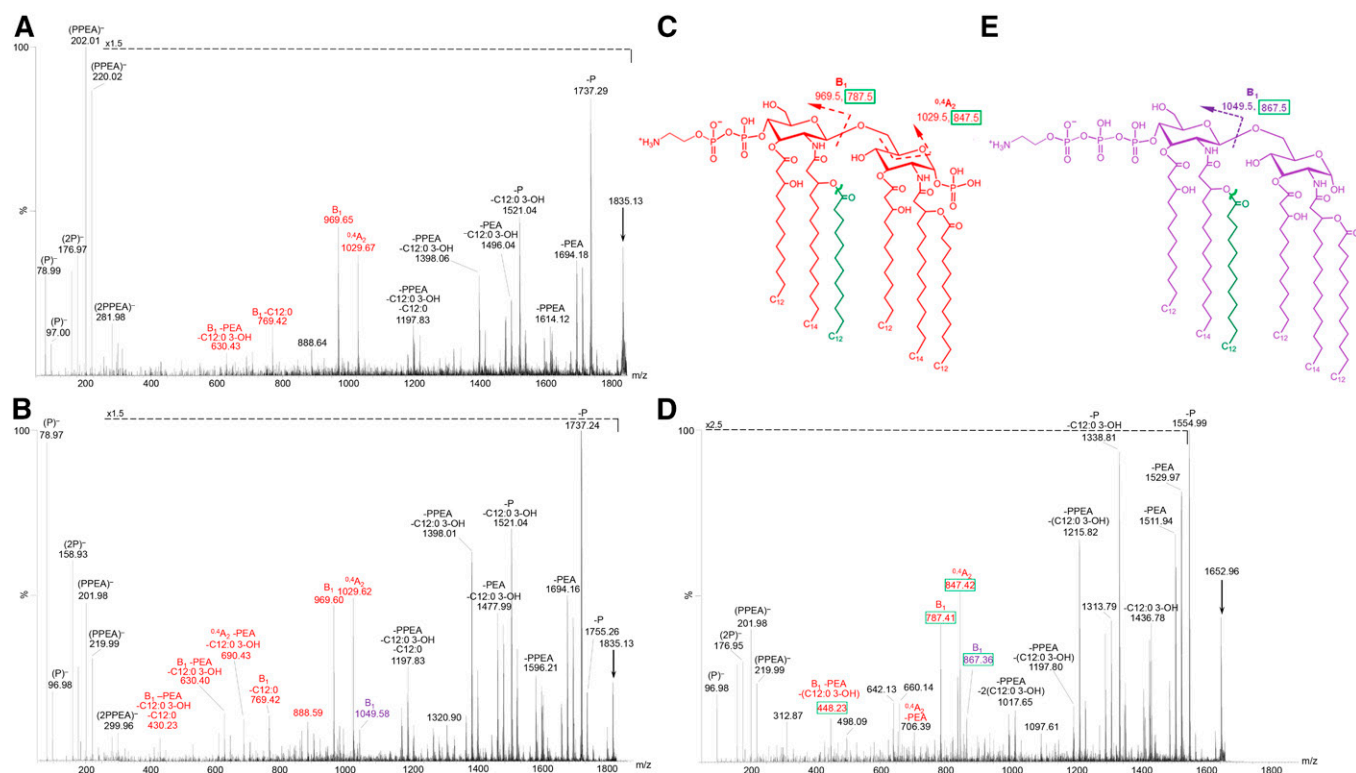


**Fig. 6.** Negative-ion MALDI-TOF IMS-MS/MS spectra of 2P PEA lipid A at  $m/z$  1,835.1 (arrows) from intact LOS of 89I (A) and 701 (B) and of 2P PEA lipid A at  $m/z$  1,653.0 from intact LOS of the 399 *lpxL1* mutant strain (D). The major fragment ions of lipid A that are informative regarding the localization of phosphoryl groups are labeled and shown on the spectra and related structures. Peaks for fragment ions due to cleavage of more than one bond are labeled in the spectra with notations for the multiple mechanisms. Corresponding structures of lipid A are presented (C, E). The color coding and labeling schemes used here are the same as described in the legend of Fig. 5.



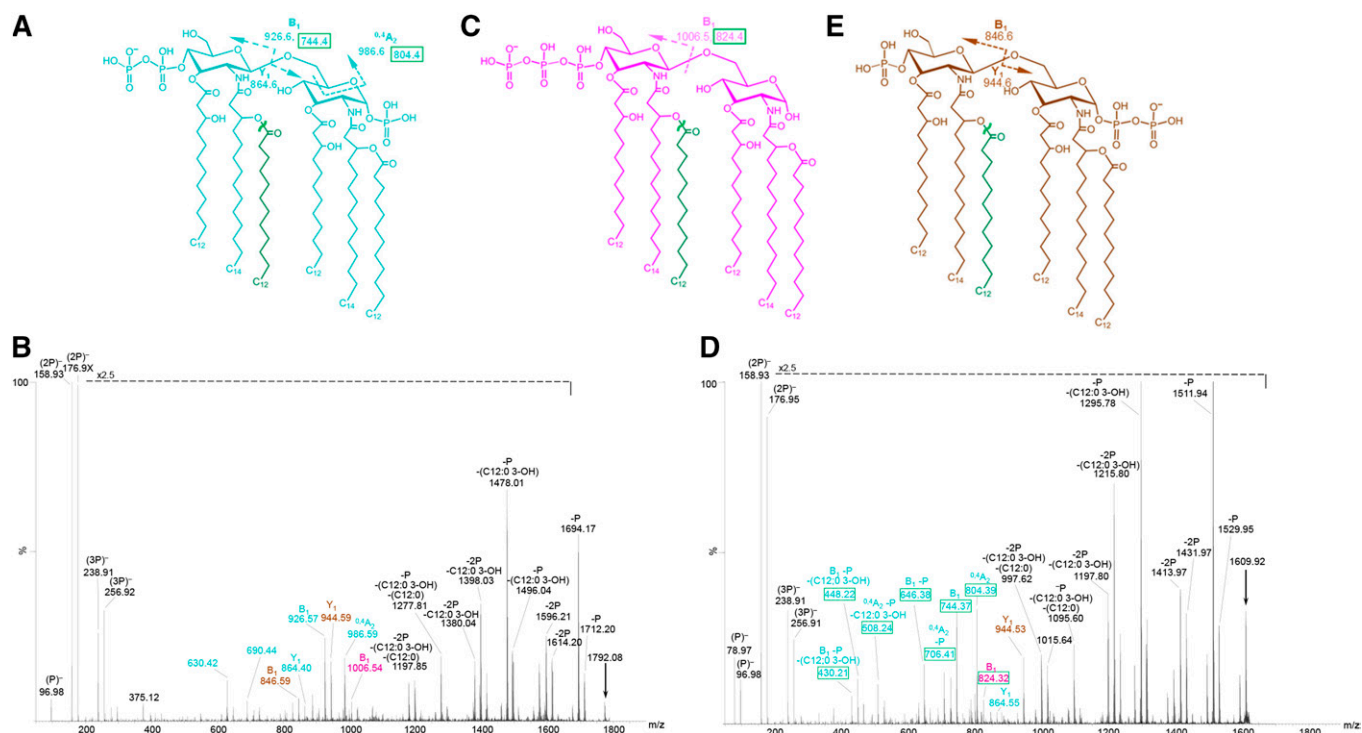


**Fig. 7.** Structures (A, C, and E) corresponding to the lipid A fragment ions detected in the negative-ion MALDI-TOF IMS-MS/MS spectra of 3P lipid A at  $m/z$  1,792.1 (arrow) from intact LOS of the 701 (B) strain and of 3P lipid A at  $m/z$  1,609.9 from intact LOS of the 399 *lpxL1* mutant strain (D). The color coding and labeling schemes used here are the same as described in the legend of Fig. 5.

by the observation of the triphosphate ions in both spectra at  $m/z$  238.9 and 256.9.

#### IMS-MS/MS of hexa-acylated and penta-acylated 3P PEA lipid A that lost $H_4P_2O_7$

Highly abundant lipid A ions were observed at  $m/z$  1,737.2 and 1,555.0 for hexa-acylated and penta-acylated lipid A, respectively, in spectra presented in Figs. 5–7. Analyses of the negative-ion MS/MS spectra of these species (supplemental Fig. S1) revealed that there were no P groups on the reducing terminus. These species likely arose through a facile fragmentation process that produced loss of a highly stable  $H_4P_2O_7$  molecule (177.94 Da) from the reducing terminus of 3P PEA lipid A as previously described (13).

#### Composite of the phosphoforms of the meningococcal lipid A

The different molecular phosphoforms detected in our IMS-MS/MS analysis of the meningococcal lipid A are summarized graphically in Fig. 8. We detected four isobaric phosphoforms of the largest 3P PEA lipid A that we investigated. The most abundant of these phosphoforms had P PEA on the nonreducing terminus and 2P on the reducing terminus. Our analysis of the 3P PEA lipid A also revealed that 2P PEA groups could be localized on either terminus with a single P on the other terminus. Some of these forms were also detected lacking P or PEA.

Of the 3P forms, we found two isobaric molecules, one with 2P on the nonreducing and P on the reducing terminus, and an additional motif with 3P on the nonreducing

terminus without P substitution on the reducing terminus. We detected no evidence for 3P reducing terminal groups or for nonreducing termini without any P.

We did not detect molecules with PEA substituents in the absence of a P on the same terminus, and we did not detect phosphoforms with symmetrical substitutions. Overall, our data indicated that there was more phosphorylation of the nonreducing glucosamine moiety compared with the reducing terminus.

## DISCUSSION

Our MALDI-TOF negative-ion MS/MS analyses of lipid A fragment ions of the Neisserial LOS that were produced by in-source decay revealed heterogeneous phosphoryl substitution. MS/MS of 3P PEA lipid A fragment ions showed that P PEA groups could be localized on either the reducing or nonreducing terminus with greater phosphoethanolaminylation of the nonreducing terminus. This is suggestive of some type of regulated biosynthetic process, albeit through differences in regiochemistry that create greater enzymatic access to the nonreducing termini or through differences in enzymatic affinity for specific lipid A acceptor molecules. Our results show that the lipid A could be pyrophosphorylated on either the 1- or the 4'-position and that PEA could be localized on the pyrophosphoryl groups on either termini. Furthermore, we identified a novel 4'-triphosphoryl lipid A. In the only other report of a triphosphoryl substituent on lipid A, it was found to be localized on the 1-position in *P. aeruginosa* LPS (22).

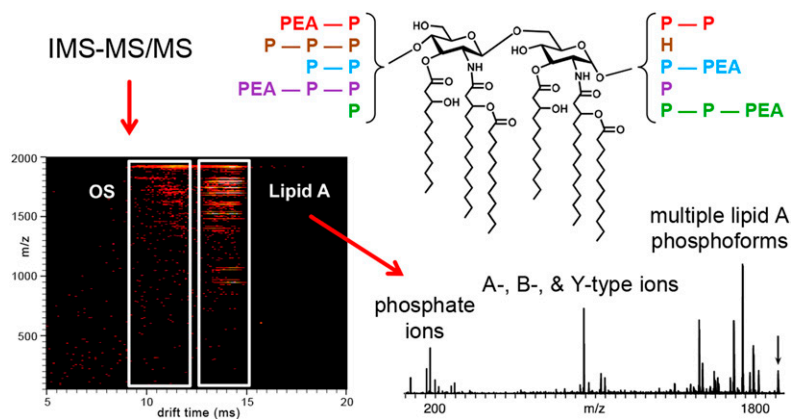


**Fig. 8.** An illustration using the mobilogram from Fig. 5B of our use of gas-phase separation with IMS-MS/MS to analyze A-, B-, and Y-type lipid A fragment ions of LOS formed in MALDI-TOF MS by in-source decay. A suite of molecules with different phosphoforms were detected that are represented on the lipid A structure using colored font to match reducing with nonreducing terminal phosphoryl substituents.

A previous structural analysis of lipid A using ESI MS/MS with transformation of *Yersinia pestis* to express either C-1 or C-4' phosphatase enzymes, LpxE and LpxF, showed that there was more loss of acyl chains as alkyl ketenes compared with alkane carboxylic acids with P at the 1-position rather than 4'-position (26). However, we could not use observation of differences in the abundance of these acyl chain fragments as a marker for localization of P on either terminus because we could not assign fragment ions as stemming from loss of acyl groups as alkane carboxylic acid or alkyl ketenes ( $\Delta 18.01$  Da). In our analysis, many fragment ions that lost acyl groups also lost P or PEA groups, which produce ions differing by 18 Da due to cleavage as  $\text{HPO}_3$  ( $-79.97$  Da) and  $\text{H}_3\text{PO}_4$  ( $-97.98$  Da) or  $\text{C}_2\text{H}_6\text{NPO}_3$  ( $-123.01$  Da) and  $\text{C}_2\text{H}_8\text{NPO}_4$  ( $-141.02$  Da), respectively.

Interestingly, in the spectrum of the penta-acylated *lpxL1* mutant strain 399 (Fig. 5H) there were significant peaks for  $B_1$  ions observed at  $m/z$  769.40 and 726.35 that had lost water from ions at  $m/z$  787.39 and 744.37, respectively, apparently through 2-bond cleavages. Similar losses of water from  $B_1$  ions were not observed in the spectra of the hexa-acylated LOS (Fig. 5D, G). It is possible that these losses of water are related to the presence of a hydroxyl group on the N-linked laurate of the nonreducing terminal glucosamine in the lipid A from the *LpxL1* mutant strain.

There are some differences in the reports regarding the effect of PEA substitution on the inflammatory potential of lipid A. Our data regarding Neisserial LOS indicate that PEA modification of the P and PP groups on the lipid A increases inflammatory signaling (12, 16). But it was reported that substitution of *bis*-phosphoryl hexa-acylated lipid A with 4-position PEA had no effect on cytokine induction in human monocytes stimulated with LPS from *Plesiomonas shigelloides* (58). Furthermore, the presence of 4-PEA on *bis*-phosphoryl hexa-acylated lipid A from *Cronobacter sakazakii* was shown to reduce NF- $\kappa$ B signaling in HEK293 cells (59), and 1-position PEA and 4-position aminoarabinose substitution of *bis*-phosphoryl hexa-acylated lipid A from *S. enterica* serovar Typhimurium also reduced inflammatory cytokine expression (60). Similarly, expression of a 1-position PEA on hexa-acylated lipid A of *Capnocytophaga canimorsus* instead of a single 1-position P decreased the NF- $\kappa$ B signaling of the bacteria in HEK293 cells (61). These differences in biological

activity indicate that the effect of PEA on inflammatory signaling could be modulated by molecular interactions dependent on other structural features of the lipid A such as, for example, the extent and localization of pyrophosphoryl groups.

We previously reported that most nonpathogenic commensal *Neisseria* express only a *bis*-phosphoryl lipid A lacking both phosphoethanolaminylation and pyrophosphorylation (16). Furthermore, we have found that differences in the extent of phosphorylation of the lipid A can be correlated with occurrence of meningococcal meningitis alone, or of septicemia with or without meningitis (5), which leads to higher mortality. Thus, we postulated that variability in phosphorylation of meningococcal lipid A could be a pivotal factor capable of tipping the balance of innate immune responses toward pro-inflammatory signaling or homeostatic tolerance and affecting adaptive immunity (62). Overall, we contend that the phosphorylation of lipid A may be an important determinant of pathogenicity in *Neisseria spp.* and is likely to play a role in maintenance of the commensal-like asymptomatic infections with *N. gonorrhoeae* and carrier states of *N. meningitidis*.

In summary, we have demonstrated that IMS-MS/MS analysis with CID of lipid A fragment ions can be used to localize phosphoryl groups on the Neisserial lipid A. Our results reveal distinct patterns of substitution with P, PP, 3P, PPEA, and 2P PEA groups. Based on the data regarding the relationship between phosphorylation and bioactivity of lipid A, variation in the immunostimulatory and inflammatory potential of the Neisserial LOS are likely to be affected by differences between the nonreducing and the reducing terminal substituents on the lipid A. We can speculate based on data on other forms of lipid A that the increased PP and PPEA substitution on the 4'-position compared with the 1-position of the lipid A could tend to decrease the inflammatory potential of the highly endotoxic LOS. More information about these unusual modifications, their bioactivity, and molecular interactions is needed to determine their role in the pathogenicity of meningococcal infections. Better understanding of the nature of and basis for the lipid A structure-activity relationships also could enable the design of new molecules that act to modulate inflammatory signaling and innate immunity.

## Data availability

All data described in the article are contained within the article. 

## Acknowledgments

The authors are grateful to Einar Rosenqvist, Norwegian Institute of Public Health, Oslo, Norway, for the *N. meningitidis* 90/90, 701, and 399 strains. The authors would also like to acknowledge National Institutes of Health/National Center for Research Resources Shared Instrumentation Grant S10 RR029446 (H. E. Witkowska) for acquisition of the Synapt G2 HDMS. This is paper number 120 from the Center for Immunochemistry.

## Author contributions

C.M.J. and N.J.P. experiments; C.M.J. and N.J.P. data analysis; C.M.J., N.J.P., and G.A.J. writing.

## Author ORCIDs

Gary A. Jarvis  <https://orcid.org/0000-0002-7576-3702>

## Funding and additional information

This work was supported by the Research Service of the United States Department of Veterans Affairs Merit Review Award BX000727 (G.A.J.). G.A.J. is the recipient of a Senior Research Career Scientist Award from the Research Service of the United States Department of Veterans Affairs.

## Conflict of interest

The authors declare that they have no conflicts of interest with the contents of this article.

## Abbreviations

CID, collision-induced dissociation; Gal, galactose; Glc, glucose; GlcN, diglucosamine; GlcNAc, *N*-acetylglucosamine; HDMS, high-definition mass spectrometer; Hep, L-glycero-D-manno-heptose; IMS, ion mobility spectrometry; Kdo, 3-deoxy-D-manno-2-octulosonic acid; LOS, lipooligosaccharide; LPS, lipopolysaccharide; MPLA, monophosphoryl lipid A; OS, oligosaccharide; P, phosphate; PEA, phosphoethanolamine; PP, pyrophosphate; PPEA, pyrophosphoethanolamine; TLR4, toll-like receptor 4.

Manuscript received July 6, 2020, and in revised form July 23, 2020. Published, JLR Papers in Press, August 24, 2020, DOI 10.1194/jlr.RA120001014.

## REFERENCES

1. Estabrook, M. M., J. M. Griffiss, and G. A. Jarvis. 1997. Sialylation of *Neisseria meningitidis* lipooligosaccharide inhibits serum bactericidal activity by masking lacto-*N*-neotetraose. *Infect. Immun.* **65**: 4436–4444.
2. Ram, S., A. D. Cox, J. C. Wright, U. Vogel, S. Getzlaff, R. Boden, J. Li, J. S. Plested, S. Meri, S. Gulati, et al. 2003. Neisserial lipooligosaccharide is a target for complement component C4b. Inner core phosphoethanolamine residues define C4b linkage specificity. *J. Biol. Chem.* **278**: 50853–50862.
3. Kahler, C. M., A. Datta, Y. L. Tzeng, R. W. Carlson, and D. S. Stephens. 2005. Inner core assembly and structure of the lipooligosaccharide of *Neisseria meningitidis*: capacity of strain NMB to express all known immunotype epitopes. *Glycobiology.* **15**: 409–419.
4. Kahler, C. M., S. Lyons-Schindler, B. Choudhury, J. Glushka, R. W. Carlson, and D. S. Stephens. 2006. *O*-Acetylation of the terminal *N*-acetylglucosamine of the lipooligosaccharide inner core in *Neisseria meningitidis*. Influence on inner core structure and assembly. *J. Biol. Chem.* **281**: 19939–19948.
5. John, C. M., N. J. Phillips, R. Din, M. Liu, E. Rosenqvist, E. A. Høiby, D. C. Stein, and G. A. Jarvis. 2016. Lipooligosaccharide structures of invasive and carrier isolates of *Neisseria meningitidis* are correlated with pathogenicity and carriage. *J. Biol. Chem.* **291**: 3224–3238.
6. Schneider, H., J. M. Griffiss, J. W. Boslego, P. J. Hitchcock, K. M. Zahos, and M. A. Apicella. 1991. Expression of paragloboside-like lipooligosaccharides may be a necessary component of gonococcal pathogenesis in men. *J. Exp. Med.* **174**: 1601–1605.
7. Tsai, C. M. 2001. Molecular mimicry of host structures by lipooligosaccharides of *Neisseria meningitidis*: characterization of sialylated and nonsialylated lacto-*N*-neotetraose (Gal $\beta$ 1–4GlcNAc $\beta$ 1–3Gal $\beta$ 1–4Glc) structures in lipooligosaccharides using monoclonal antibodies and specific lectins. *Adv. Exp. Med. Biol.* **491**: 525–542.
8. Cochet, F., and F. Peri. 2017. The role of carbohydrates in the lipopolysaccharide (LPS)/Toll-like receptor 4 (TLR4) signalling. *Int. J. Mol. Sci.* **18**: 2318.
9. Zughair, S. M., Y. L. Tzeng, S. M. Zimmer, A. Datta, R. W. Carlson, and D. S. Stephens. 2004. *Neisseria meningitidis* lipooligosaccharide structure-dependent activation of the macrophage CD14/Toll-like receptor 4 pathway. *Infect. Immun.* **72**: 371–380.
10. Zughair, S., S. Agrawal, D. S. Stephens, and B. Pulendran. 2006. Hexa-acylation and KDO<sub>2</sub>-glycosylation determine the specific immunostimulatory activity of *Neisseria meningitidis* lipid A for human monocyte derived dendritic cells. *Vaccine.* **24**: 1291–1297.
11. Mandrell, R. E., J. J. Kim, C. M. John, B. W. Gibson, J. V. Sugai, M. A. Apicella, J. M. Griffiss, and R. Yamasaki. 1991. Endogenous sialylation of the lipooligosaccharides of *Neisseria meningitidis*. *Bacteriol.* **173**: 2823–2832.
12. John, C. M., M. Liu, and G. A. Jarvis. 2009. Profiles of structural heterogeneity in native lipooligosaccharides of *Neisseria* and cytokine induction. *J. Lipid Res.* **50**: 424–438.
13. Jones, J. W., S. A. Shaffer, R. K. Ernst, D. R. Goodlett, and F. Turecek. 2008. Determination of pyrophosphorylated forms of lipid A in Gram-negative bacteria using a multivariate mass spectrometric approach. *Proc. Natl. Acad. Sci. USA.* **105**: 12742–12747.
14. John, C. M., M. Liu, and G. A. Jarvis. 2009. Natural phosphoryl and acyl variants of lipid A from *Neisseria meningitidis* strain 89I differentially induce tumor necrosis factor- $\alpha$  in human monocytes. *J. Biol. Chem.* **284**: 21515–21525.
15. Liu, M., C. M. John, and G. A. Jarvis. 2010. Phosphoryl moieties of lipid A from *Neisseria meningitidis* and *N. gonorrhoeae* lipooligosaccharides play an important role in activation of both MyD88- and TRIF-dependent TLR4-MD-2 signaling pathways. *J. Immunol.* **185**: 6974–6984.
16. John, C. M., M. Liu, N. J. Phillips, Z. Yang, C. R. Funk, L. I. Zimmerman, J. M. Griffiss, D. C. Stein, and G. A. Jarvis. 2012. Lack of lipid A pyrophosphorylation and of a functional *lptA* reduce inflammation by *Neisseria* commensals. *Infect. Immun.* **80**: 4014–4026.
17. Cox, A. D., J. C. Wright, J. Li, D. W. Hood, E. R. Moxon, and J. C. Richards. 2003. Phosphorylation of the lipid A region of meningococcal lipopolysaccharide: identification of a family of transferases that add phosphoethanolamine to lipopolysaccharide. *J. Bacteriol.* **185**: 3270–3277.
18. Anandan, A., G. L. Evans, K. Condic-Jurkic, M. L. O'Mara, C. M. John, N. J. Phillips, G. A. Jarvis, S. S. Wills, K. A. Stubbs, I. Moraes, et al. 2017. Structure of a lipid A phosphoethanolamine transferase suggests how conformational changes govern substrate binding. *Proc. Natl. Acad. Sci. USA.* **114**: 2218–2223.
19. Kahler, C. M., K. L. Nawrocki, A. Anandan, A. Vrielink, and W. M. Shafer. 2018. Structure-function relationships of the Neisserial EptA enzyme responsible for phosphoethanolamine decoration of lipid A: rationale for drug targeting. *Front. Microbiol.* **9**: 1922.
20. Samantha, A., and A. Vrielink. 2020. Lipid A Phosphoethanolamine Transferase: Regulation, Structure and Immune Response. *J. Mol. Biol.* **432**: 5184–5196.
21. Herrera, C. M., J. V. Hankins, and M. S. Trent. 2010. Activation of PmrA inhibits LpxT-dependent phosphorylation of lipid A promoting resistance to antimicrobial peptides. *Mol. Microbiol.* **76**: 1444–1460.

22. Nowicki, E. M., J. P. O'Brien, J. S. Brodbelt, and M. S. Trent. 2014. Characterization of *Pseudomonas aeruginosa* LpxT reveals dual positional lipid A kinase activity and coordinated control of outer membrane modification. *Mol. Microbiol.* **94**: 728–741.
23. Scia drone, B., F. Forti, S. Perego, F. Falchi, and F. Briani. 2019. Temperature-dependent regulation of the *Escherichia coli* lpxT gene. *Biochim. Biophys. Acta. Gene Regul. Mech.* **1862**: 786–795.
24. Lamarche, M. G., S. H. Kim, S. Crépin, M. Mourez, N. Bertrand, R. E. Bishop, J. D. Dubreuil, and J. Harel. 2008. Modulation of hexa-acyl pyrophosphate lipid A population under *Escherichia coli* phosphate (Pho) regulon activation. *J. Bacteriol.* **190**: 5256–5264.
25. Pridmore, A. C., G. A. Jarvis, C. M. John, D. L. Jack, S. K. Dower, and R. C. Read. 2003. Activation of toll-like receptor 2 (TLR2) and TLR4/MD2 by *Neisseria* is independent of capsule and lipooligosaccharide (LOS) sialylation but varies widely among LOS from different strains. *Infect. Immun.* **71**: 3901–3908.
26. Jones, J. W., I. E. Cohen, F. Turecek, D. R. Goodlett, and R. K. Ernst. 2010. Comprehensive structure characterization of lipid A extracted from *Yersinia pestis* for determination of its phosphorylation configuration. *J. Am. Soc. Mass Spectrom.* **21**: 785–799.
27. Beutler, B. 2000. Tlr4: central component of the sole mammalian LPS sensor. *Curr. Opin. Immunol.* **12**: 20–26.
28. Park, B. S., D. H. Song, H. M. Kim, B. S. Choi, H. Lee, and J. O. Lee. 2009. The structural basis of lipopolysaccharide recognition by the TLR4-MD-2 complex. *Nature.* **458**: 1191–1195.
29. Ohto, U., K. Fukase, K. Miyake, and T. Shimizu. 2012. Structural basis of species-specific endotoxin sensing by innate immune receptor TLR4/MD-2. *Proc. Natl. Acad. Sci. USA.* **109**: 7421–7426.
30. Zughair, S. M., S. M. Zimmer, A. Datta, R. W. Carlson, and D. S. Stephens. 2005. Differential induction of the toll-like receptor 4-MyD88-dependent and -independent signaling pathways by endotoxins. *Infect. Immun.* **73**: 2940–2950.
31. Duncan, J. A., X. Gao, M. T. Huang, B. P. O'Connor, C. E. Thomas, S. B. Willingham, D. T. Bergstralh, G. A. Jarvis, P. F. Sparling, and J. P. Ting. 2009. *Neisseria gonorrhoeae* activates the proteinase cathepsin B to mediate the signaling activities of the NLRP3 and ASC-containing inflammasome. *J. Immunol.* **182**: 6460–6469.
32. Knodler, L. A., S. M. Crowley, H. P. Sham, H. Yang, M. Wrande, C. Ma, R. K. Ernst, O. Steele-Mortimer, J. Celli, and B. A. Vallance. 2014. Noncanonical inflammasome activation of caspase-4/caspase-11 mediates epithelial defenses against enteric bacterial pathogens. *Cell Host Microbe.* **16**: 249–256.
33. Viganò, E., C. E. Diamond, R. Spreafico, A. Balachander, R. M. Sobota, and A. Mortellaro. 2015. Human caspase-4 and caspase-5 regulate the one-step non-canonical inflammasome activation in monocytes. *Nat. Commun.* **6**: 8761.
34. Lewis, L. A., B. Choudhury, J. T. Balthazar, L. E. Martin, S. Ram, P. A. Rice, D. S. Stephens, R. Carlson, and W. M. Shafer. 2009. Phosphoethanolamine substitution of lipid A and resistance of *Neisseria gonorrhoeae* to cationic antimicrobial peptides and complement-mediated killing by normal human serum. *Infect. Immun.* **77**: 1112–1120.
35. Balthazar, J. T., A. Gusa, L. E. Martin, B. Choudhury, R. Carlson, and W. M. Shafer. 2011. Lipooligosaccharide structure is an important determinant in the resistance of *Neisseria gonorrhoeae* to antimicrobial agents of innate host defense. *Front. Microbiol.* **2**: 30.
36. Kandler, J. L., S. J. Joseph, J. T. Balthazar, V. Dhulipala, T. D. Read, A. E. Jerse, and W. M. Shafer. 2014. Phase-variable expression of *lptA* modulates the resistance of *Neisseria gonorrhoeae* to cationic antimicrobial peptides. *Antimicrob. Agents Chemother.* **58**: 4230–4233.
37. Packiam, M., R. D. Yedery, A. A. Begum, R. W. Carlson, J. Ganguly, G. D. Sempowski, M. S. Ventevogel, W. M. Shafer, and A. E. Jerse. 2014. Phosphoethanolamine decoration of *Neisseria gonorrhoeae* lipid A plays a dual immunostimulatory and protective role during experimental genital tract infection. *Infect. Immun.* **82**: 2170–2179.
38. Takahashi, H., R. W. Carlson, A. Muszynski, B. Choudhury, K. S. Kim, D. S. Stephens, and H. Watanabe. 2008. Modification of lipooligosaccharide with phosphoethanolamine by LptA in *Neisseria meningitidis* enhances meningococcal adhesion to human endothelial and epithelial cells. *Infect. Immun.* **76**: 5777–5789.
39. Coats, S. R., A. B. Berezow, T. T. To, S. Jain, B. W. Bainbridge, K. P. Banani, and R. P. Darveau. 2011. The lipid A phosphate position determines differential host Toll-like receptor 4 responses to phylogenetically related symbiotic and pathogenic bacteria. *Infect. Immun.* **79**: 203–210.
40. Casella, C. R., and T. C. Mitchell. 2008. Putting endotoxin to work for us: monophosphoryl lipid A as a safe and effective vaccine adjuvant. *Cell. Mol. Life Sci.* **65**: 3231–3240.
41. Mata-Haro, V., C. Cekic, M. Martin, P. M. Chilton, C. R. Casella, and T. C. Mitchell. 2007. The vaccine adjuvant monophosphoryl lipid A as a TRIF-biased agonist of TLR4. *Science.* **316**: 1628–1632.
42. Coats, S. R., J. W. Jones, C. T. Do, P. H. Braham, B. W. Bainbridge, T. T. To, D. R. Goodlett, R. K. Ernst, and R. P. Darveau. 2009. Human Toll-like receptor 4 responses to *P. gingivalis* are regulated by lipid A 1- and 4'-phosphatase activities. *Cell. Microbiol.* **11**: 1587–1599.
43. Fukuoka, S., K. Brandenburg, M. Muller, B. Lindner, M. H. Koch, and U. Seydel. 2001. Physico-chemical analysis of lipid A fractions of lipopolysaccharide from *Erwinia carotovora* in relation to bioactivity. *Biochim. Biophys. Acta.* **1510**: 185–197.
44. Phillips, N. J., C. M. John, and G. A. Jarvis. 2016. Analysis of bacterial lipooligosaccharides by MALDI-TOF MS with traveling wave ion mobility. *J. Am. Soc. Mass Spectrom.* **27**: 1263–1276.
45. Kogan, G., D. Uhrin, J. R. Brisson, and H. J. Jennings. 1997. Structural basis of the *Neisseria meningitidis* immunotypes including the L4 and L7 immunotypes. *Carbohydr. Res.* **298**: 191–199.
46. Bjune, G., E. A. Høiby, J. K. Gronnesby, O. Arnesen, J. H. Fredriksen, A. Halstensen, E. Holten, A. K. Lindbak, H. Nøkleby, E. Rosenqvist, et al. 1991. Effect of outer membrane vesicle vaccine against group B meningococcal disease in Norway. *Lancet.* **338**: 1093–1096.
47. Høiby, E. A., G. Bjune, L. O. Frøholm, J. Eng, A. Halstensen, E. Rosenqvist, E. Ronnild, and E. Wedege. 1991. The Norwegian meningococcal serogroup B outer membrane vesicle vaccine protection trials: case tracing, meningococcal antigen detection and serological diagnosis. *NIPH Ann.* **14**: 107–121.
48. Frøholm, L. O., D. A. Caugant, E. Holten, E. A. Høiby, E. Rosenqvist, and E. Wedege. 1991. Meningococcal strains isolated from teenage patients during the serogroup B vaccination trial in Norway: serotyping, serosubtyping, immunotyping and clonal analysis. *NIPH Ann.* **14**: 139–143.
49. Apicella, M. A., J. M. Griffiss, and H. Schneider. 1994. Isolation and characterization of lipopolysaccharides, lipooligosaccharides, and lipid A. *Methods Enzymol.* **235**: 242–252.
50. Westphal, O., and K. Jann. 1965. Bacterial lipopolysaccharides extraction with phenol-water and further applications of the procedure. In *Methods in Carbohydrate Chemistry*. Vol. 5. Academic Press Inc., London. 83–91.
51. Stephenson, H. N., C. M. John, N. Naz, O. Gundogdu, N. Dorrell, B. W. Wren, G. A. Jarvis, and M. Bajaj-Elliott. 2013. *Campylobacter jejuni* lipooligosaccharide sialylation, phosphorylation, and amide/ester linkage modifications fine-tune human Toll-like receptor 4 activation. *J. Biol. Chem.* **288**: 19661–19672.
52. Sturiale, L., D. Garozzo, A. Silipo, R. Lanzetta, M. Parrilli, and A. Molinaro. 2005. New conditions for matrix-assisted laser desorption/ionization mass spectrometry of native bacterial R-type lipopolysaccharides. *Rapid Commun. Mass Spectrom.* **19**: 1829–1834.
53. Giles, K., S. D. Pringle, K. R. Worthington, D. Little, J. L. Wildgoose, and R. H. Bateman. 2004. Applications of a travelling wave-based radio-frequency-only stacked ring ion guide. *Rapid Commun. Mass Spectrom.* **18**: 2401–2414.
54. Pringle, S. D., K. Giles, J. L. Wildgoose, J. P. Williams, S. E. Slade, K. Thalassinou, R. H. Bateman, M. T. Bowers, and J. H. Scrivens. 2007. An investigation of the mobility separation of some peptide and protein ions using a new hybrid quadrupole/travelling wave IMS/oa-ToF instrument. *Int. J. Mass Spectrom.* **261**: 1–12.
55. Kulshin, V. A., U. Zahringer, B. Lindner, C. E. Frasch, C. M. Tsai, B. A. Dmitriev, and E. T. Rietschel. 1992. Structural characterization of the lipid A component of pathogenic *Neisseria meningitidis*. *J. Bacteriol.* **174**: 1793–1800.
56. van der Ley, P., L. Steeghs, H. J. Hamstra, J. ten Hove, B. Zomer, and L. van Alphen. 2001. Modification of lipid A biosynthesis in *Neisseria meningitidis* lpxL mutants: influence on lipopolysaccharide structure, toxicity, and adjuvant activity. *Infect. Immun.* **69**: 5981–5990.
57. Domon, B., and C. Costello. 1988. A systematic nomenclature for carbohydrate fragmentations in FAB-MS/MS spectra of glycoconjugates. *Glycoconj. J.* **5**: 397–409.
58. Kaszowska, M., M. Wojcik, J. Siednienko, C. Lugowski, and J. Lukasiewicz. 2017. Structure-activity relationship of *Plesiomonas*

- shigelloides* lipid A to the production of TNF- $\alpha$ , IL-1 $\beta$ , and IL-6 by human and murine macrophages. *Front. Immunol.* **8**: 1741.
59. Liu, L., Y. Li, X. Wang, and W. Guo. 2016. A phosphoethanolamine transferase specific for the 4'-phosphate residue of *Cronobacter sakazakii* lipid A. *J. Appl. Microbiol.* **121**: 1444–1456.
60. Aldapa-Vega, G., M. A. Moreno-Eutimio, A. J. Berlanga-Taylor, A. P. Jiménez-Urbe, G. Nieto-Velazquez, O. López-Ortega, I. Mancilla-Herrera, E. M. Cortés-Malagon, J. S. Gunn, A. Isibasi, et al. 2019. Structural variants of *Salmonella* Typhimurium lipopolysaccharide induce less dimerization of TLR4/MD-2 and reduced pro-inflammatory cytokine production in human monocytes. *Mol. Immunol.* **111**: 43–52.
61. Renzi, F., U. Zahringer, C. E. Chandler, R. K. Ernst, G. R. Cornelis, and S. J. Ittig. 2015. Modification of the 1-phosphate group during biosynthesis of *Capnocytophaga canimorsus* lipid A. *Infect. Immun.* **84**: 550–561.
62. John, C. M., N. J. Phillips, D. C. Stein, and G. A. Jarvis. 2017. Innate immune response to lipooligosaccharide: pivotal regulator of the pathobiology of invasive *Neisseria meningitidis* infections. *Pathog. Dis.* **75**: doi:10.1093/femspd/ftx030.